Journal of The Electrochemical Society, **155** (12) D791-D797 (2008)
0013-4651/2008/155(12)/D791/7/$23.00 © The Electrochemical Society

Defect-Free Copper Filling Using Nonisothermal Electroless Deposition with Fluorocarbon Surfactant

Yu-Hsien Chou,[a] Yuh Sung,[b] Yih-Ming Liu,[c] Nen-Wen Pu,[c] and Ming-Der Ger[c,*,z]

[a]*Graduate School of Defense Science, Chung Cheng Institute of Technology, National Defense University, Tao-Yuan, Taiwan*
[b]*Chung Shan Institute of Science and Technology, Tao-Yuan, Taiwan*
[c]*Department of Applied Chemistry & Materials Science, Chung Cheng Institute of Technology, National Defense University, Tao-Yuan, Taiwan*

Electroless copper bottom-up filling of patterned substrates using nonisothermal deposition (NITD) with the addition of adequate surfactant was demonstrated. Combining the inhibitive ability of adequate surfactant with the higher driving force of NITD method, superfill of vias or trenches using only one inhibitor in the copper damascene of integrated circuits (ICs) was achieved. We tested several commercial surfactant agents and found that fluorinated alkyl quaternary ammonium iodides (FC) is best compatible to our NITD method. Void-free copper-filled features can be obtained by introducing the surfactant FC into the electroless bath of NITD. Furthermore, using our method, the conductivity of copper film was not negatively affected. We conclude that the surfactant FC combined with NITD method is very promising for the applications in filling trenches and vias with copper films in the IC industry.
 [DOI: 10.1149/1.2999368]

Manuscript submitted July 24, 2008; revised manuscript received September 18, 2008. Published October 21, 2008.

Electroless plating can deposit a metal film from an ionic solution onto catalytic sites of a substrate without any external power supply and has been widely applied to microelectronic packaging and manufacturing of integrated circuits (ICs).[1-6] It has also received great attention for its lower tool cost, excellent step-coverage capability for via holes and trenches, lower process temperature, and capability to deposit a metal film on a nonconductive specimen after sensitization and activation treatments.[7-9]

Copper is now used in place of conventional aluminum-based wiring in ultralarge-scale integrated logic devices. Its outstanding advantages of low electrical resistivity (1.67 $\mu\Omega$ cm), high melting point (1085°C), and superior resistance against electromigration are very desirable for the electronic industry.[10,11] Moreover, copper electroless plating is a premium process to deposit copper lines or seedlayers in the process of IC patterning before copper electroplating.

However, there are three often-seen problems in the technique of electroless plating. First, it needs to activate the barrier/SiO_2/Si substrate using palladium (Pd) before copper electroless plating. The resistivity of Pd is ~10 $\mu\Omega$ cm, and the temperature of some ordered solid solution phases of Cu–Pd are below 500°C. Therefore, in the copper damascene process, the interdiffusion of Pd into copper easily form an alloy that increases the resistivity and the resistance-capacitance delay effect during the postannealing process.[12,13] Second, the difficulty to control the unstable deposition reaction resulting from inadequate concentration of stabilizer is common in typical electroless plating. Keeping a constant quantity of stabilizer is also difficult in the process.[14,15] Third, with the increase of IC density and the shrinkage in IC dimension, completely stuffing the submicrometer or nanometer features becomes more and more important, and is always a difficult issue during the copper deposition process. When the aspect ratio (a ratio of trench depth to its width) is >3, voids or seams are usually inevitable in the filling, and to stuff the high-aspect-ratio trenches or via holes void freely or seamlessly with electroless plating is difficult.[16] Superfilling or bottom-up filling can only be procured for high aspect ratio microstructures when the deposition rate at the bottom of feature is higher than that at the corners of opening. Using additives, such as polyethylene glycol (PEG), Tritton-100, RE-610, bis(3-sulfopropyl) disulfide (SPS), 8-hydroxy-7-iodo-5-quinoline sulfonic acid, and mercapto alkyl carboxylic acid, in an electroless solution has always been expected to get better deposition characteristics for the superfilling of copper.[16-22] The void-free or seamless-filling pattern was attained by electroless plating using two or more additives, some of which are accelerators and others are inhibitors (or suppressors), in the plating bath. Although the problems of voids or seams embedded in the deposition film could be solved by adding accelerators and inhibitors, the conductivity of copper will be negatively affected by the impurities that result from the hydrolysate of these additives. To solve this problem, Shingubara et al. recently used a suppressing agent, SPS, to achieve bottom-up filling of Cu.[17] Lee et al. also achieved void-free filling by using SPS as a suppressing-accelerating agent.[23] In addition, they also used an additive, 3-*N*, *N*-dimethylaminodithiocarbamoly-1-propanesulfonic acid, as a suppressing-accelerating agent to perform the copper bottom-up filling.[24]

In this study, a technology named nonisothermal deposition (NITD) method is proposed to provide a way for the superfill of copper electroless plating. Our previous study[25-30] indicated that the NITD method is able to efficiently create nanoparticles by spontaneous nucleation and deposit these nanoparticles on the substrate. Meanwhile, it can enhance the stability of plating bath without using stabilizers and still keep a high deposition rate. Addtionally, the NTID method, which can deposit metal thin film in one step, has extra advantages in discarding the catalytic noble metal and simplifying the deposition processes.

We have tested several commercial surfactants, such as PEG, SPS, polyoxyethylene nonylphenyl ether [CO-890, $(C_2H_4O)_nC_{15}H_{24}O$ from 3M Co.], and fluorinated alkyl quaternary ammonium iodides [(FC), (FC-134) from 3M Co.], to find out which one is best compatible to our NITD method. After extensive tests and evaluation, surfactant FC was proved to have good inhibiting ability to perform bottom-up filling and to maintain a smoother surface of the deposited film. Combining the high deposition rate of NITD method and the good inhibiting ability of surfactant FC, superfilling of trenches with copper at a satisfactory rate was achieved in this study. The superfill mechanism was explained by a nonlinear diffusion phenomenon of the surfactant FC. Moreover, the electrochemistry, morphology, and resistivity of deposited thin copper films were also evaluated.

Experiments

The substrates we used in this study were blank p-type (100) Si wafers (boron doped with a resistivity of 10–20 Ω cm), micrometer-patterned silicon wafers (with aspect ratios of 2.9 and 2.3), and submicrometer-patterned silicon wafers (with aspect ratios of 1, 1.3, and 5.5) that use TaN grown by ionized metal plasma as a barrier layer, respectively. Prior to electroless copper plating, all substrates

* Electrochemical Society Active Member.
[z] E-mail: mdger@ccit.edu.tw

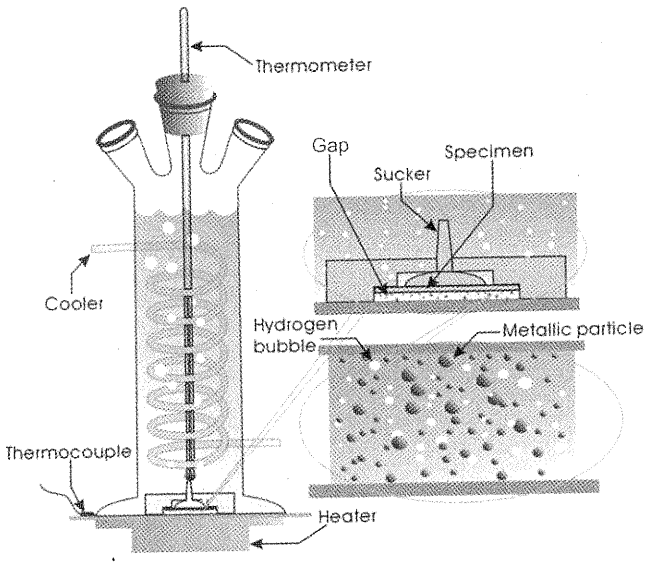

Figure 1. Schematic diagram of the NITD system, in which white and gray dots represent hydrogen bubbles and metal-precipitated nanoparticles, respectively.

were cleaned by ultrasound in acetone for 5 min at room temperature, rinsed with Super Q DI, and then dried by nitrogen gas purge.

Direct electroless copper plating onto the inert substrates without using Pd activation was performed in NITD system.[26-31] The NITD method is designed to selectively reduce metal ions only within a heating zone in the gap between the heater and the substrate, as shown in Fig. 1. This reactor is constructed of a heater, a temperature controller, a thermostat, and a glass vessel including a helix cooler. The substrate, which was bonded closely with the heater, was fixed on the bottom of the reactor so that its operating temperature allowed precise control. The temperature of plating bath (T_b) can be flexibly adjusted with the cooling system cased outside the reactor. On the basis of this design, the deposition temperature of the substrate (T_s) and bath (T_b) can be operated independently, and T_s, in general, was operated much higher than T_b. The higher T_s could enhance the reaction rate in electroless plating bath; in the meantime, the lower T_b can keep electrolyte stable for a longer bath life. The gap between the heater and the plate substrate is adjustable. The mass and heat transfer in the gap will be significantly different from those in the bath because the gap was only set at 150 μm. In our past study,[25] we used EG&G/PAR 263 potentiostat/galvanostat with the CorWare and CorView software to estimate the temperature distribution in the heating gap between substrate and heater. The results showed that the thickness of a uniform reaction zone between substrate and heater is ~755 μm when T_s is 120°C. Because the gap of the NITD system in this study is set at 150 μm and the depth of the tiny patterns is <30 μm, it is reasonable to assume that the thermal gradient in the reaction zone is unapparent.

The electrolyte solution consisted of copper sulfate ($CuSO_4 \cdot 2H_2O$), ethylenediaminetetraacetic acid (Na_2EDTA), and formaldehyde. The pH value was adjusted to 12.5 using NaOH. The effects of adding surfactants PEG (molecular weight or MW = 400), SPS (MW = 304), CO-890 (MW = 484), FC (MW = 364), etc., on deposition characteristics were investigated. The range of deposition temperature was between 100 and 120°C. The composition of solution and the operating conditions of this experiment are shown in Table I. The bath temperature (T_b) is adjusted by the cooling system. The temperature of substrate (T_s) was controlled by the heater and the thermocouple. After the copper electroless deposition, these substrates were rinsed, dried, and then examined.

The interfacial structure and filling features in cross-sectional patterned wafers were observed by the field emission scanning electron microscope (FE-SEM). The surface topography of the formed film was examined by tapping-mode atomic force microscopy (AFM), which measures the average roughness (Ra) in a square of 9 μm^2. The electrical resistivity of the deposited copper film was probed by a four-point probe method. The reactions between the copper surface and surfactants of various concentrations were scanned by an EG&G/PAR 263 potentiostat/galvanostat with the CorWare and CorView software. The electrochemical experiments were performed using a typical three-electrode cell. The working electrode consisted of a pure copper sheet (99.99% purity). The counter electrode was a platinum sheet, and all potentials were recorded with respect to an Ag/AgCl electrode. Measurements were implemented at room temperature in the electrolyte of formaldehyde solution. The sweep range of formaldehyde oxidation potential was from −1.0 to 0 V and then back to −1.0 V.

Table I. Bath components and operating conditions.

Copper $SO_4 \cdot 5H_2O$	14.981 g/L
Na_2EDTA	35.0 g/L
HCHO	10 mL/L
Surfactants (PEG, Co-890, SPS and FC)	10–100 mg/L
Volume	100 mL
pH (adjusted with NaOH)	12.5
deposition time	5 min, 10 min, and 1 h
T_s	100 and 120°C
T_b	10°C

Results and Discussion

The schematic diagram of the mechanism of NITD is shown in Fig. 2. In the initial stage of deposition, as seen in Fig. 2a, the reduction of metal ions proceeded steadily within a gap near the heated platform, which was at a high deposition temperature, and then the reduced nuclei diffused from the designed space toward the substrate by thermal diffusion and convection. In Fig. 2b, the copper seed layer was produced by the continuous adsorption of these nuclei to the substrate, and then the follow-up reduction of copper ions was catalyzed by this seed layer. Because the inhibiting effect on the corners was more distinct than that on the bottom due to the larger amount of FC absorbed on the corners, the deposition rate of copper on the bottom was higher than that on the corners, as shown in Fig. 2c. Finally, a well-bonded and void-free copper conductor was formed after a period of reactive time, as seen in Fig. 2d. The three

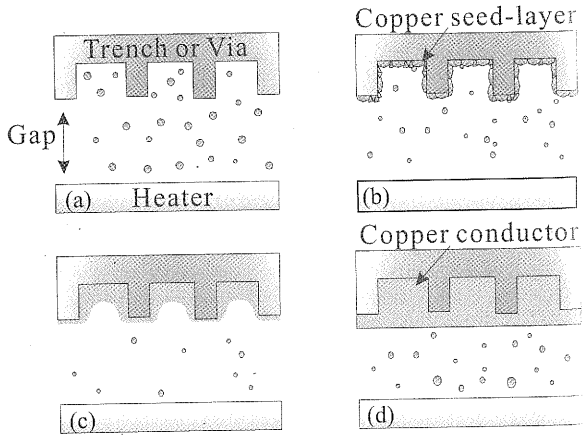

Figure 2. Schematic diagram presenting the copper deposition process during NITD reaction: (a) nucleation and diffusion of these nuclei, (b) copper seed layer formation, (c) copper layer growth, and (d) formation of copper conductor in which the gray dots represents copper nuclei.

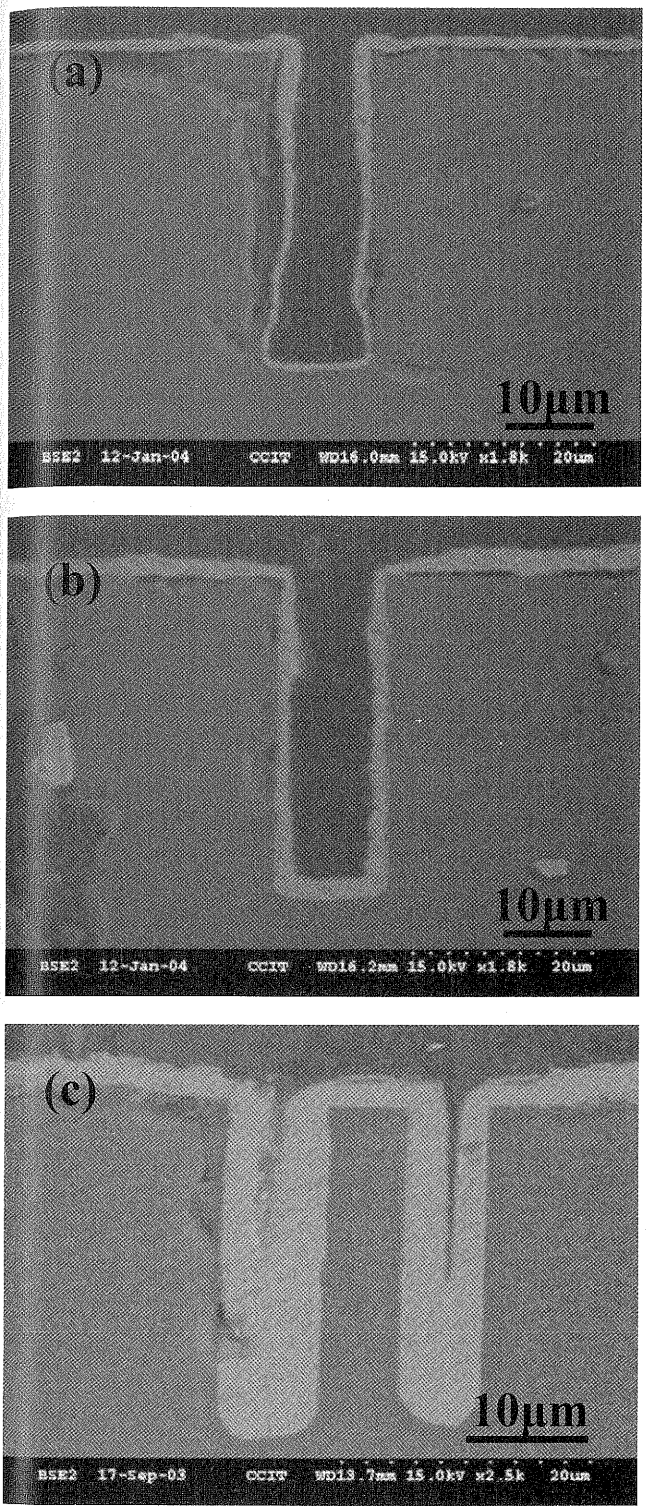

Figure 3. Cross-sectional SEM images of copper-filled via holes deposited for various deposition times by NITD: (a) 5, (b) 10, and (c) 30 min. The deposition/cooling temperatures were 120°C/20°C, and the surfactant concentration was 40 mg/L.

SEM images for sequential transient feature filling were shown in Fig. 3. The deposition times for Fig. 3a-c were 5, 10, and 30 min, respectively.

In the study, we have investigated the effects of various surfactants (CO-890, PEG, SPS, and FC) on the bottom-up filling characteristics of electroless copper plating solution to fill the micrometer via-hole patterns. The electroless copper plating with an NITD system was performed with the same gap width, deposition temperature, and concentration of surfactant. Furthermore, the copper films were deposited without any typical catalyst, which were dissimilar to those formed by conventional deposition processes needing sensitization and activation. The different inhibition effects of the sufactants (CO-890, PEG, SPS, and FC) on the flat Si wafer surface are shown in Fig. 4, which consists of a series of AFM three-dimensional (3D) images of thin copper films obtained, respectively, by depositing with 40 mg/L CO-890, PEG, SPS, or FC, at a deposition temperature of 120°C. The Ra of these copper films are 20.8, 25.3, 32.8, and 7.9 nm in Fig. 4a-d, respectively. The surface morphology of the deposited film will be drastically affected by the inhibiting effect of surfactants. For example, if the surfactant has better inhibiting capability, the surface roughness of deposited film will apparently decrease and the granule sizes will be more uniform. The copper film in Fig. 4d, showing the minimum Ra (7.9 nm) and the most uniform granule size among the four samples, reveals that the surfactant FC has the best inhibitive capacity among these surfactants. Figures 5a-c indicate that the voids existed in the entire depth when the surfactants CO-890, PEG, or SPS were added into the deposition solution. The formation of voids in the patterns of Fig. 5a-c can be attributed to the overgrowth of edges resulting from the nonlinear diffusion of the chemical species at the entrance corners of the hole.[31-34] It reveals that these surfactants (CO-890, PEG, and SPS) adsorbed at the entrance of the via hole were insufficient to alleviate the copper overgrowth in the electroless deposition because of their poor inhibiting effect. The superconformal filling occurred only in the case of FC, as depicted in Fig. 5d, indicating that the surfactant FC has excellent inhibitive capacity to alleviate the reaction of electroless copper deposition at the entrance of the via hole. However, the high driving force in the NITD system can still keep the deposition rate on the bottom high enough to achieve super filling. The SPS stacked on the corners and outside surface of the specimen even sped up the electroless copper deposition, as shown in Fig. 5c.

In the copper damascene process, chemical-mechanical polishing (CMP) is usually employed to remove the uneven copper deposit and flatten the wafer surface. However, it is easy to cause localized defects of copper dishing and dielectric erosion, or keep the contaminations at the interface of interconnects during CMP. The addition of surfactant FC in the electroless copper bath not only resolves the tough problem of void in the via but also lessens the damage of IC-device from the CMP process, because the thickness of copper film on the surface of feature is thinner and thus the time for CMP can be reduced.

Figure 6 shows the ratio of film thickness at the bottom of the via to that at the outside surface, or the "bottom-top ratio" CT_b/CT_s, (CT_b: copper film thickness at the bottom of via hole, CT_s: copper film thickness at the outside surface of pattern) of electrolessly deposited copper in NITD method using various surfactants. The bottom-top ratios are 0.86, 0.38, 0.09, and 9.33, respectively, for CO-890, PEG, SPS, and FC. The bottom-up filling mechanism was due to the effect of the inhibitor, which was adsorbed largely on the entrance corners of the pattern to inhibit the copper overgrowth. Furthermore, because of the concentration gradient of chemical species, the inhibitor cannot diffuse sufficiently into the bottom of the via hole to hinder the copper deposition. The copper deposition is appreciably influenced by the inter-reaction among copper ions, formaldehyde, surfactant, and other species in the electroless bath. In the SPS bath, the bottom-top ratio was the smallest. It had been demonstrated that the surfactant SPS accelerated the deposition rate of copper film on the entrance even with low concentration.[35] In the bath of FC, the bottom-top ratio increased because the amount of FC adsorbed at the entrance was larger than at the bottom by the rationale of nonlinear mass diffusion. As a result, the deposition of electroless copper is alleviated at the entrance due to the excessive inhibition with surfactant FC. Overgrowth of copper film at the entrance corners of high aspect ratio and small entrance pattern was

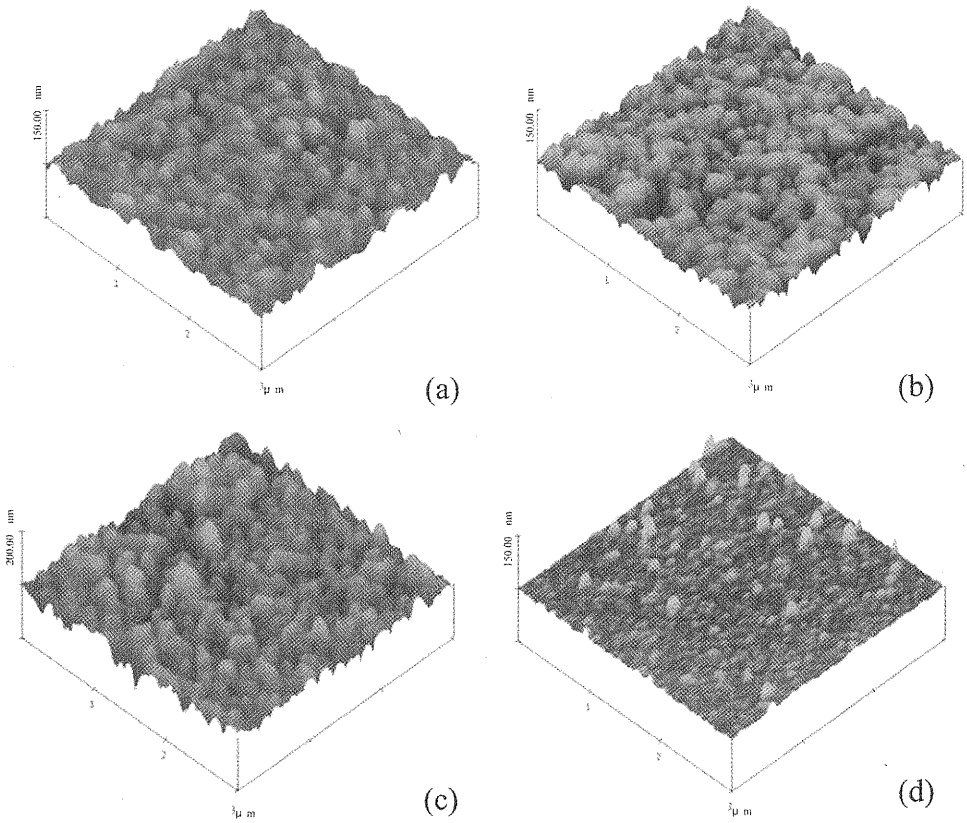

Figure 4. (Color online) Variation of the 3D AFM surface morphology of copper films deposited using various surfactants with 40 mg/L at the deposition/cooling temperatures of 120°C/20°C (3 × 3 μm): (a) CO-890 (Ra = 20.8 nm), (b) PEG (Ra = 25.3 nm), (c) SPS (Ra = 32.8 nm), and (d) FC (Ra = 7.9 nm). According to the order of the roughness of copper film, the ranking of inhibition capability of surfactant is FC > CO-890 > PEG > SPS.

believed to block the chemical species from diffusing into the tiny hole or trench, resulting in a void-embedded filling. Therefore, inhibiting the deposition rate of copper at the entrance corners while still keeping a higher deposition rate at the bottom of the pattern by an effective surfactant and its gradient distribution may be the solution to achieve superfilling. A similar mechanism for this bottom-up filling behavior proposed by Shingubara et al. is the leveling theory by diffusion controlled adsorption of inhibitor molecules (SPS) on the Cu surface.[17]

The surfactant FC could be considered as a more effective inhibitor than the other three surfactants to prevent the metal film deposition from overgrowth at the entrance. An important viewpoint

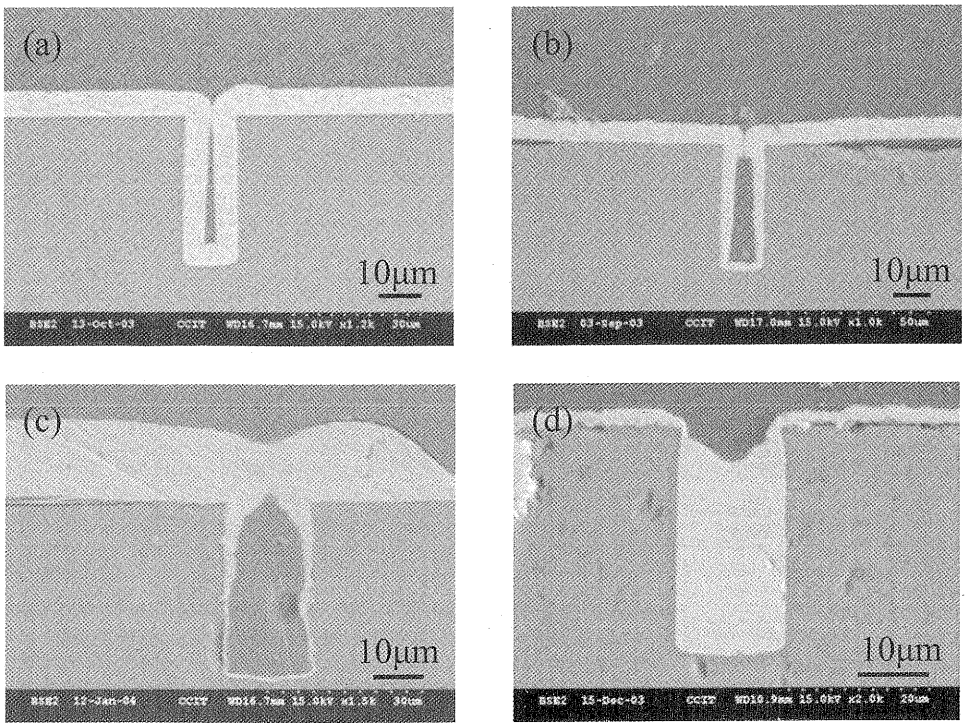

Figure 5. Cross-sectional SEM images of copper-filled via holes deposited with various surfactants in NITD method for plating time of 1 h, deposition/cooling temperatures of 120°C/20°C, concentration level of surfactant at 40 mg/L. (a) CO-890, bottom width: 13 μm, depth: 38 μm, aspect ratio: 2.9; (b) PEG, bottom width: 13 μm, depth: 38 μm, aspect ratio: 2.9; (c) SPS, bottom width: 17 μm, depth: 38 μm, aspect ratio: 2.3; and (d) FC, bottom width: 15 μm, depth: 34 μm, aspect ratio: 2.3.

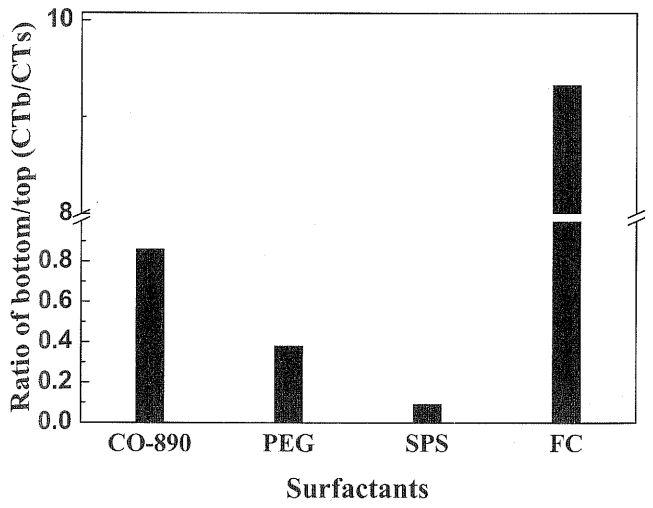

Figure 6. The bottom-top ratio of electrolessly deposited copper in NITD method using various surfactants. Plating time is 1 h. Deposition/cooling temperatures are 120°C/20°C. Surfactant concentration is 40 mg/L.

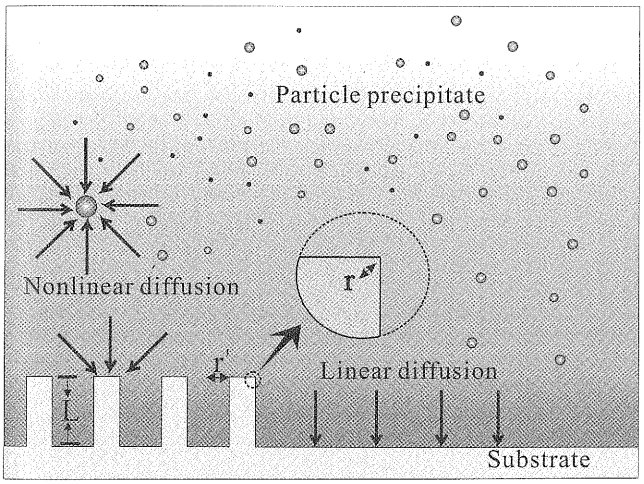

Figure 7. Schematic diagram presenting the diffusion phenomena of chemicals with respect to tiny features or platform substrate.

emphasizes the fact that when FC was adsorbed on the corners of the feature, it could effectively hinder the nonlinear mass diffusion of copper deposit due to its excellent inhibiting effect. The metal film deposition may thus be expected to have an anisotropic growth in the microstructure patterning.[36]

Figure 7 and Eq. 1-3 can elucidate how the surfactant shielded the nonlinear mass diffusion of the copper deposit. Equations 1-3 are the mass flux equations for the species in the electroless plating bath[37]

$$J = \frac{DC_0}{\delta} \quad [1]$$

$$J' = \frac{DC_0}{\delta} + \frac{4DC_0}{\pi r} \quad [2]$$

$$J'' = \frac{DC_0}{\delta} + \frac{DC_0}{r' + L} \quad [3]$$

where D is the diffusion coefficient, C_0 is the chemical concentration in bulk solution, δ is the thickness of the diffusion layer, r is the curvature radius of the tiny feature, r' is the radius of microstructure, and L is the depth of microstructure. Equations 1-3 and Fig. 7 describe the diffusion phenomena of surfactant FC at different microstructures in the electroless plating bath. Generally, J denotes the mass flux on the panel, J' denotes the mass flux on the tiny substrates (such as nanoparticle or the entrance corners of microstructure), and J'' denotes the mass flux in the recessed features (such as via hole or trench), respectively. When $r \gg \delta$, the species will diffuse like on a large flat, and J' will be equal to J. Hence, the diffusion flux J' will be equal to J and result in linear diffusion, as seen in Fig. 7. Whereas, if the radius r is so small that its behavior is similar to that on nanoparticles or at the entrance corners of tiny pattern, as shown in Fig. 7, the diffusion flux J' will be larger than J and result in a nonlinear diffusion. From this viewpoint, the FC was adsorbed predominately onto the entrance corners of tiny pattern than the plate substrate and alleviated the metal deposition on the corners. In addition, Eq. 3 relates to the depth of the microstructure. As the aspect ratio of microstructure is large ($L \gg r'$), it is very difficult for diffusion flux to reach the bottom of the deep hole. Therefore, FC diffuses less into the bottom than to the entrance of microstructure, which is predominately governed by the concentration gradient that can be completely determined with these diffusive equations.

Figure 8 shows the schematic diagram of copper deposition at the entrance of via hole in the FC-added bath and FC-free bath, respectively. The void is observed in the via holes when deposited in the FC-free bath. The formation of void is attributed to overgrowth of edges contributed from nonlinear diffusion of the copper deposit

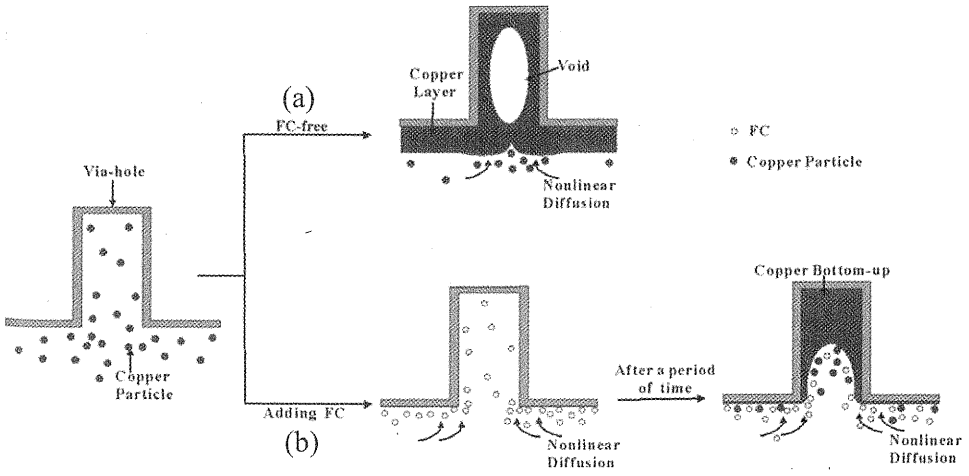

Figure 8. Schematic diagram of the copper deposition at a via hole: (a) without and (b) with surfactant FC in the electroless copper bath.

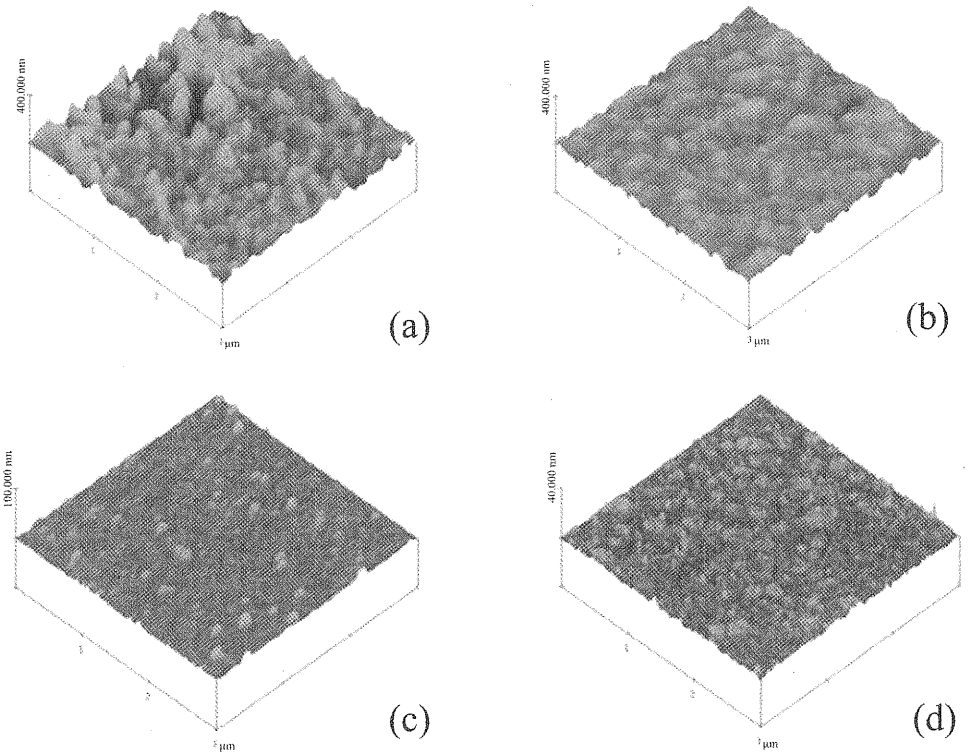

Figure 9. (Color online) Variation of the 3D AFM surface morphology of copper films as a function of FC concentration at the deposition/cooling temperatures of 100°C/20°C and plated for 5 min (3 × 3 μm): (a) 0 mg/L (Ra = 79.8 nm), (b) 25 mg/L (Ra = 39.2 nm), (c) 50 mg/L (Ra = 4.584 nm), and (d) 100 mg/L (Ra = 1.596 nm).

at the entrance corners of the hole. The inhibition of FC is effective on both the "precipitation" of copper particles and the "electroless deposition" of copper at the surface. What makes the superfilling-type deposition was that the inhibitor (FC) was adsorbed largely on the entrance corners of pattern rather than on the bottom by nonlinear diffusion. Furthermore, the high driving force in the NITD system can still keep the Cu deposition rate high on the bottom, which was not severely affected by the inhibitor, and achieve superfilling.

Figure 9 shows a series of AFM 3D images of thin copper films obtained, respectively, from four concentrations of FC at the deposition temperature of 100°C. The average roughnesses (Ra) of these copper films are 79.8, 39.2, 4.6, and 1.6 nm when deposited with 0, 25, 50, and 100 mg/L of FC, respectively. The surface morphology of copper film was drastically affected by the FC concentration: the surface roughness was apparently reduced and the grain size was more uniform as the concentration of FC increased. This indicates that the excellent inhibitive capacity of surfactant FC can also reduce the surface roughness of the deposited copper film, which is helpful for the superfilling application on the submicron structures.

In order to verify the above-mentioned phenomenon that surfactant FC possesses great ability to be adsorbed onto the copper film and silicon wafer, we demonstrate it with a well-known cyclic voltammetry. Figure 10 shows the cycles of the voltammogram profiles in formaldehyde solutions having various concentrations of FC. The peak of anodic current corresponds to the oxidation of the formaldehyde catalyzed by the copper specimen. In the solution of formaldehyde without FC (curve A), the negative potential sweep showed a well-defined anodic current peak at ca −0.31 V. When the solution was added with 50 mg/L FC, the current of the peak (curve B) decreased relative to the FC-free electrolyte solution. An inhibiting effect was observed (i.e., FC was adsorbed onto the copper surface and significantly eliminated the activity of the catalytic sites at the copper surface). When the concentration of FC was promoted to 100 mg/L (curve C), an inhibiting effect made the limiting current even less and shifted the potential of the peak to the left. In addition, at high concentration of FC (e.g., 500 mg/L) (curve D), the most drastic inhibiting effect in our experiments was observed. The oxidative behavior of the D peak was not the same as others, that is to say, the peak disappeared completely and the current density of the oxidation was minimized. The above phenomena can be associated with the rigid adsorption of FC on the copper film, where all of the reactive sites were almost blocked by the quasi-inhibitor.[6] As a result, the cycles of the voltammograms demonstrated that FC can drastically adsorb onto the corners and the surface of microstructures to inhibit available copper deposition. The negative peak in the current density appeared at −0.6 V when FC is increased. Because the chemical reaction is so complicated, the variation of this negative peak needs to be further verified.

In order to prepare the trench-filling copper, we added 50 mg/L FC into the electroless bath, and the cross-sectional FE-SEM image of copper deposit was shown in Fig. 11. The trench widths of the patterned wafer were 0.1 μm (aspect ratio is 5.5), 0.5 μm (aspect ratio is 1.1), and 0.4 μm (aspect ratio is 1.3), respectively. The trenches were successfully filled without voids and seams forming in the pattern. It is attractive that copper can be completely depos-

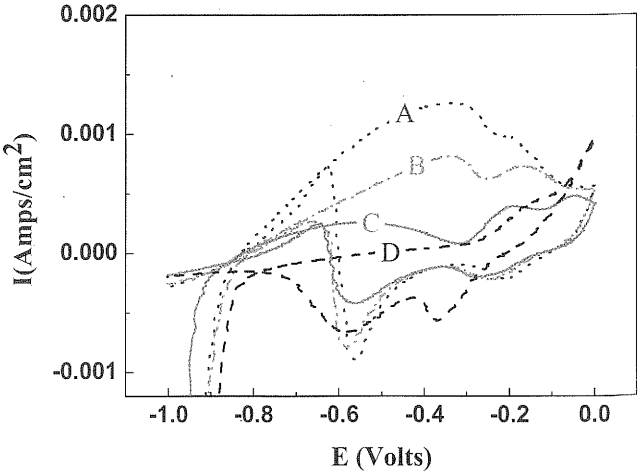

Figure 10. (Color online) A typical diagram of cyclic voltammetry at the formaldehyde bath with different concentrations of FC (A: 0, B: 50, C: 100, and D: 500 mg/L).

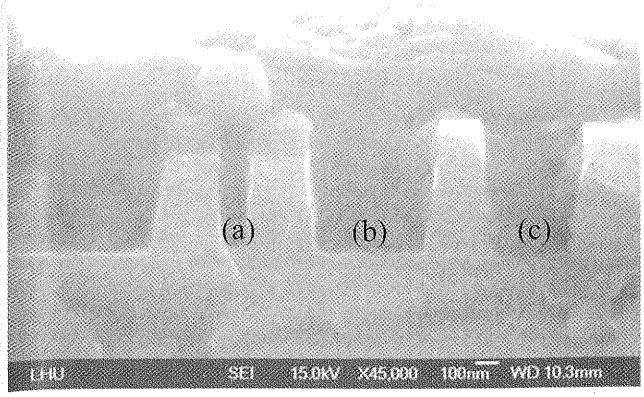

Figure 11. Cross-sectional FE-SEM image of the copper filled in the trench deposited with the addition of 50 mg/L FC, plating time of 10 min, at deposition/cooling temperatures of 120°C/20°C. (a) bottom width: 0.1 μm, depth: 0.55 μm, aspect ratio: 5.5; (b) bottom width: 0.5 μm, depth: 0.55 μm, aspect ratio: 1.1; and (c) bottom width: 0.4 μm, depth: 0.55 μm, aspect ratio: 1.3.

ited into the trenches or vias by NITD method without any pretreatment of activation and copper seed layer. According to the aforementioned results, void-free copper deposits used for interconnects can be successfully achieved by means of the NITD method and the quasi-inhibitor.

The resistivity of as-deposited copper films with various FC concentration levels is shown in Fig. 12. The film thickness of each sample was maintained at about 200 ± 10 nm. Without adding surfactant FC, the resistivity of as-deposited copper film is ~4.1 μΩ cm. The higher resistivity may be attributed to the stacked structure of nanoparticles and some nanoscale voids embedded in the film. As the FC concentration increases from 0 to 100 mg/L, the resistivity of copper film increases slightly. The FC additive does not significantly affect the resistivity of copper film as compared to those deposited without FC. It may result from the high cloud point of FC (>100°C), which prevented FC from hydrolyzing into F and

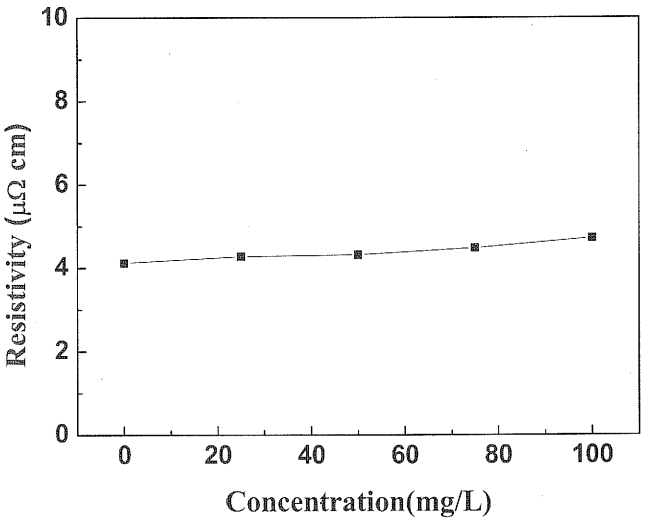

Figure 12. The measured electrical resistivity of the as-deposited copper films as a function of the concentration of FC. Plating time: 1, 1.5, 3, 4.5, and 6.5 min for the solutions with 0, 25, 50, 75, and 100 mg/L FC, respectively. Deposition/cooling temperatures: 120°C/20°C.

C elements and being embedded in the copper deposit. However, the more detailed mechanism needs to be further verified.

Conclusion

In this paper, we demonstrate the feasibility of direct electroless plating of copper on patterned silicon wafer in the NITD system, without the need to catalyze the surface using any activation treatment. Because of the robust inhibition capability of surfactant FC, submicrometer trenches were successfully filled by electroless copper deposition. The conformal trench-filling copper conductor was achieved in electroless copper plating bath added with 50 mg/L FC. This void-free filling was achieved due to the inhibiting effect of FC at the corners of trench. Moreover, adding surfactant FC into the NITD bath did not appreciably impact the resistivity of deposited copper films and the surface roughness of the copper film declined significantly when the FC concentration increased.

Acknowledgment

The authors acknowledge the financial support from the National Science Council of Taiwan under grant no. NSC-93-2214-E-014-002.

University of National Defense assisted in meeting the publication costs of this article.

References

1. J. W. Schultze and A. Bressel, *Electrochim. Acta*, **47**, 3 (2001).
2. T. Homma, I. Komatsu, A. Ttamaki, H. Nakai, and T. Osaka, *Electrochim. Acta*, **47**, 47 (2001).
3. T. Hara, S. Kamijima, and Y. Shimura, *Electrochem. Solid-State Lett.*, **6**, C8 (2003).
4. H. H. Hsu, C. W. Teng, S. J. Lin, and J. W. Yeh, *J. Electrochem. Soc.*, **149**, C143 (2002).
5. Y. Morand, *Microelectron. Eng.*, **50**, 391 (2000).
6. P. C. Andricacos, C. Uzoh, J. O. Dukovic, J. Horkans, and H. Deligianni, *IBM J. Res. Dev.*, **42**, 567 (1998).
7. N. Feldstein and P. Amodio, *J. Electrochem. Soc.*, **117**, 1110 (1970).
8. H. H. Hsu, C. W. Teng, S. J. Lin, and J. W. Yeh, *J. Electrochem. Soc.*, **149**, C143 (2002).
9. S. W. Hong, C. H. Shin, and J. W. Park, *J. Electrochem. Soc.*, **149**, G85 (2002).
10. S. P. Murarka, *Mater. Sci. Eng., R.*, **R19**, 87 (1997).
11. T. Homma, *Thin Solid Films*, **278**, 28 (1996).
12. P. R. Subramanian and D. E. Laughlin, *J. Phase Equilib.*, **12**, 231 (1991).
13. N. E. Lay, G. A. Ten Eyck, D. J. Duquette, and T. M. Lu, *Electrochem. Solid-State Lett.*, **10**, D13 (2007).
14. J. Shu, B. P. A. Grandjean, and S. Kaliaguine, *Ind. Eng. Chem. Res.*, **36**, 1632 (1997).
15. R. T. Morrison and R. N. Boyd, *Organic Chemistry*, 5th ed. New York University, Allyn & Bacon, Inc., Boston (1987).
16. Z. Wang, R. Obata, H. Sakaue, T. Takahagi, and S. Shingubara, *Electrochim. Acta*, **51**, 2442 (2006).
17. S. Shingubara, Z. Wang, S. Yaegashi, R. Obata, H. Sakaue, and T. Takahagi, *Electrochem. Solid-State Lett.*, **7**, C78 (2004).
18. Y. Shacham-Diamand and S. Lopatain, *Microelectron. Eng.*, **37/38**, 77 (1997).
19. V. M. Dubin, Y. Shacham-Diamand, B. Zhao, P. K. Vasudev, and C. H. Ting, *J. Electrochem. Soc.*, **144**, 898 (1997).
20. M. Tan and J. N. Harb, *J. Electrochem. Soc.*, **150**, C420 (2003).
21. M. Kang and A. A. Gewirth, *J. Electrochem. Soc.*, **150**, C426 (1997).
22. M. Hasegawa, Y. Okinaka, Y. Shacham-Diamand, and T. Osaka, *Electrochem. Solid-State Lett.*, **9**, C138 (2006).
23. C. H. Lee, S. C. Lee, and J. J. Kim, *Electrochim. Acta*, **50**, 3563 (2005).
24. C. H. Lee, S. K. Cho, and J. J. Kim, *Electrochem. Solid-State Lett.*, **8**, J27 (2005).
25. M. D. Ger, Y. Sung, and J. L. Ou, *Mater. Chem. Phys.*, **89**, 383 (2005).
26. Y. Sung, M. D. Ger, Y. H. Chou, *J. Mater. Sci. Lett.*, **22**, 1515 (2003).
27. Y. Sung and M. D. Ger, *J. Chin. Inst. Chem. Eng.*, **34**, 531 (2003).
28. J. L. Ou, Y. Y. Shan, Y. Sung, Y. H. Chou, and M. D. Ger, *J. Chin. Soc. Mech. Eng.*, **26**, 729 (2005).
29. Y. Sung, J. L. Ou, M. D. Ger, and Y. H. Chou, in *New Developments in Material Science Research*, edited by B. M. Caruta, Chap. 1, Nova, New York (2007).
30. Y. M. Liu, M. J. Shieh, Y. Sung, and M. D. Ger, *Mater. Chem. Phys.*, **106**, 399 (2007).
31. A. M. T. Van der Putten and J. W. G. de Bakker, *J. Electrochem. Soc.*, **140**, 2221 (1993).
32. S. Zhang, J. De Baets, M. Vereeken, A. Vervae, and A. Van Calster, *J. Electrochem. Soc.*, **146**, 2870 (1999).
33. J. W. M. Jacobs and J. M. G. Rikken, *J. Electrochem. Soc.*, **135**, 2822 (1988).
34. N. Feldstein and P. Amodio, *J. Electrochem. Soc.*, **117**, 1110 (1970).
35. R. Akolkar and U. Landauz, *J. Electrochem. Soc.*, **151**, C702 (2004).
36. K. L. Lin and C. H. Wu, *J. Electrochem. Soc.*, **150**, C273 (2003).
37. M. Madou, *Fundamentals of Microfabrication*, CRC Press, Boca Raton (1997).